OPTIMIZATION OF PERIODIC TRUSS MATERIALS BY NIAH HOMOGENIZATION METHOD AND METAMODELING

Sandmara Lanhi

Marco Antônio Luersen

sandmara_lanhi@hotmail.com

luersen@utfpr.edu.br

Universidade Tecnológica Federal do Paraná (UTFPR)

Rua Deputado Heitor Alencar Furtado, 5000, 81280-340, Paraná, Curitiba, Brasil

Pablo Andrés Muñoz-Rojas

pablo.amr@gmail.com

Universidade do Estado de Santa Catarina (UDESC)

Rua Paulo Malschitzki, 200, 89219-710, Santa Catarina, Joinville, Brasil

Abstract. *The rapid technological evolution requires, more and more, the development of low-weight materials able of withstanding high loads. A class of materials that has stood out due to its properties is the materials consisting of lattice cells. These ones are structured so that their unit cell is repeated many times, forming a periodic material. However, obtaining the effective properties of these materials can be costly and difficult, due to the complexity of their microstructure. Therefore, this work aims to use the novel implementation of asymptotic homogenization (NIAH) to obtain the effective elastic and thermal properties of these materials. The NIAH is combined with an optimization technique based on Kriging metamodeling to reduce the computational time during the optimization process, since the evaluation of the objective function can be costly. A sequential quadratic programming algorithm (SQP) is used as the local optimizer, associated with an infill strategy. Cross sectional areas are adopted as design variables, keeping the relative density constant. Examples of cases studies are the maximization of the shear modulus and the maximization of the thermal conductivity in the x direction.*

Keywords: *Periodic truss materials, Homogenization, Metamodeling.*

Proceedings of the XXXVIII Iberian Latin-American Congress on Computational Methods in Engineering P.O. Faria, R.H. Lopez, L.F.F. Miguel, W.J.S. Gomes, M. Noronha (Editores), ABMEC, Florianópolis, SC, Brazil, November 5-8, 2017.

1 INTRODUCTION

In the design of engineering structures, it is common to choose a material and use it in the best possible way, changing their dimensions or shape. Another option is to combine different materials making a composite, opening new ways for the design of more efficient structures, taking advantage of the high stiffness/weight ratio and anisotropy of such materials. With this, recently a new approach for the design of structures has been proposed by various researchers. It is suggested to adapt the microstructure of the material for a particular application. That is, the material is designed specifically for the loading condition to which it will be subjected. Examples of materials arisen from this approach are the cellular materials.

Cellular materials are composed of voids distributed in a matrix. The matrix can be polymeric, ceramic or metallic and the material is classified according to the size of their cell (stochastic or periodic), the pore type (open or closed) and the relative density of the structure (Wadley, 2002). Usually, can also have 20% or less of their weight occupied by solid material (Ashby et al., 2000).

Among these materials, the most outstanding class is the materials consisting of lattice cells, called lattice block materials (LBM) or periodic truss materials (PTM). These belong to the class of ultralight materials and they have a periodic structure. The main reasons that lead to the wide use of these materials are due to their high strength/weight ratio and too high capacity for kinetic energy absorption, enhanced vibrational and damping characteristics, acoustic noise attenuation, shear strength, fracture strength, and directional heat conduction or insulation (Muñoz-Rojas et al., 2010). LBM show less dispersion in their physical properties when compared to other classes of cell materials of the same relative density, such as stochastic structure materials, called stochastic foams.

However, obtaining the physical properties of such materials is difficult because of a large quantity of heterogeneities present in their structure and their complexity microstructure. Thus, a common approach used for the analysis of these materials is to take its macrostructure as a homogeneous material. For this, only one of its unit cells is analyzed in order to find the effective properties of the material as a whole. These properties can be used in a later stage in the modeling of the macrostructure, but now having the model as homogeneous and without considering the microstructure, thus reducing computational time.

To find the effective properties of these materials, several methods have been proposed. However, one of the most used is the method of asymptotic homogenization (AH). This method has a rigorous mathematical foundation based on the perturbation theory and, through this, the effective properties are obtained by solving partial equations defined on a unit cell. However, AH is a method that requires time in the resolution of the equations by finite elements. In addition, for each type of element chosen to model the cell, the finite element formulation must be modified (Cheng et al., 2013).

To overcome the problems related to the use of the AH method, the researchers Cheng et al. (2013), developed a new implementation for the asymptotic homogenization (NIAH) method. This new implementation is based on the traditional method, however, it uses commercial finite element software in the modeling of the unit cell and calculations of displacements, forces, temperatures and heat flows, making all the work by finite elements be

performed by the software. In addition, it allows different types of elements to be used to discretize the cell, without changing the code formulation.

Thus, this work aims to use the new implementation of asymptotic homogenization to obtain the effective properties of materials consisting of lattice cells. In addition, it is sought to optimize the unit cells in order to obtain better thermomechanical responses. Examples of cases studies are the maximization of the shear modulus and the maximization of the thermal conductivity in the x direction. For this, cross-sectional areas are used as design variables. In the optimization process, a metamodel technique, called Kriging, is used in order to reduce the computational time. The sequential quadratic programming algorithm (SQP) is employed as a local optimizer, associated with an infill strategy to iteratively update the model and increase the efficiency of the algorithm in the search for global optima.

2 PERIODIC MATERIAL

According to Hassani et al. (1998), a material is classified as periodic if the functions that determine its physical or geometric quantities respect the following relation:

$$\mathcal{F}(\mathbf{x} + \mathbf{NY}) = \mathcal{F}(\mathbf{x}), \tag{1}$$

where $\mathcal{F}$ is the physical property in question, which can be a scalar, a vector or a tensorial, $\mathbf{x} = [x_1, x_2, x_3]^T$ is the position vector for any point **x**, **N** is a diagonal matrix of 3x3 dimension of arbitrary integers, which has the form:

$$\mathbf{N} = \begin{bmatrix} n_1 & 0 & 0 \\ 0 & n_2 & 0 \\ 0 & 0 & n_3 \end{bmatrix} \tag{2}$$

and $\mathbf{Y} = [Y_1, Y_2, Y_3]^T$ is the vector of constant values that represents the dimensions of the cell (cell period).

The **Y** period, when compared to the global domain dimensions, assumes very small values. Consequently, the characteristic functions of these highly heterogeneous media will rapidly vary within a very small neighborhood of a point **x**. Because of this, two different dependency scales must be taken into account for all quantities: one indicates the macroscopic or global scale, *x*, which represents slow variations and the other indicates the microscale or local level *y*, which represents rapid oscillations (Hassani et al., 1998).

The relation between these two dependency scales is through a small parameter ε, called the characteristic dimension of heterogeneity and is given by:

$$y = \frac{x}{\varepsilon}. \tag{3}$$

As mentioned earlier, the characteristic functions of these materials vary slightly in a very small neighborhood of any point **x**, making it difficult to obtain the effective properties of these materials. However, this can be avoid using the homogenization method. In this method, the properties in the macro scale are obtained in an approximate way, ignoring the microstructure in the global analysis, in order to simplify the analysis (Sigmund, 1994).

3 ASYMPTOTIC HOMOGENIZATION METHOD

The homogenization, from the mathematical point of view, is a theory of limits that use asymptotic expansion and assumption of periodicity. This is used to substitute the differential equations for fast oscillation coefficients, with differential equations whose coefficients are constant or vary slowly so that the solutions are close to the initial equations (Hassani et al., 1998). This theory has been used successfully in the determination of the homogenized properties of periodical materials in two and three dimensions, analytically and numerically. In addition, this technique can be applied to different areas of physics and engineering with finely continuous and heterogeneous media, such as heat transfer or fluid flow in porous media, or electromagnetism in composites.

Based on the theory presented in Hassani et al. (1998), Hassani et al. (1999), Guth (2012), Muñoz-Rojas et al. (2010) and Guedes et al. (1989), in the following subsections, the equation for determining the homogenized elastic tensor and the thermal conductivity matrix for LBM is briefly presented.

3.1 Homogenization of elastic constitutive tensor

Based on the AH theory, the effective homogenized properties for the periodic material shown schematically in Fig. 1 can be determined by assuming that the asymptotically expanded double displacement field is equal to:

$$\mathbf{u}(\mathbf{x},\mathbf{y}) = \mathbf{u}_0(\mathbf{x}) + \varepsilon\mathbf{u}_1(\mathbf{x},\mathbf{y}), \tag{4}$$

where the subscripts 0 and 1 represent the macro and microscale, respectively.

The homogenized equation is obtained and the effective coefficients are determined by the solution of the equation

$$\int_Y E_{ijpq}\frac{\partial \chi_p^{kl}}{\partial y_p}\frac{\partial v_i}{\partial y_j}dY = \int_Y E_{ijkl}\frac{\partial v_i}{\partial y_j}dY, \tag{5}$$

where E_{ijkl} is the elastic modulus of material in the unit cell, χ_p^{kl} (k, l, p $\in$\{1,2,3\} for 3D and \{1,2\}for 2D) is the characteristic displacement, v_i is test displacement and Y is the unit cell domain. The characteristic displacement is solution of the unit cell, applied with uniform unit strain and periodic boundary conditions (Cheng et al., 2013).

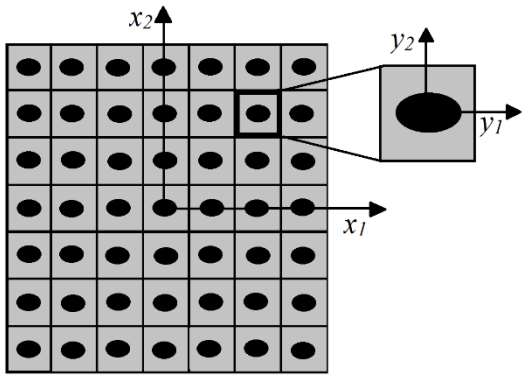

Figure 1. Periodic material and corresponding unit cell.

Thus, by rearranging Eq. (5), the homogenized elastic tensor can be obtained by

$$E^H_{ijkl}(\mathbf{x}) = \frac{1}{|\mathbf{Y}|}\int_{\mathrm{Y}} \left(E_{ijkl} - E_{ijpq}\frac{\partial \chi^{kl}_p}{\partial y_q} \right) \mathrm{dY}, \tag{6}$$

where $|\mathbf{Y}|$ is the volume of the unit cell.

However, to obtain the homogenized elastic tensor, it is necessary to solve Eq. (5) and Eq. (6) using the finite element method applying periodic boundary conditions at the cell boundaries. In practice, to obtain the solution of Eq. (5) the characteristic displacement of the cell must be found, which is obtained by:

$$\mathbf{K}\boldsymbol{\chi}^{kl} = \mathbf{f}^{kl}, \tag{7}$$

where

$$\mathbf{K} = \int_Y \mathbf{B}^T \mathbf{E} \mathbf{B}\, dY, \tag{8}$$

$$\mathbf{f}^{kl} = \int_Y \mathbf{B}^T \mathbf{E} \boldsymbol{\varepsilon}^{0(\mathrm{kl})}\, dY, \tag{9}$$

the term **K** is the global stiffness matrix, **B** is the finite element strain-displacement matrix, **E** is the constitutive matrix, **f** is the global force vector and **ε** corresponds to three (2D) or six (3D) unit strain fields. For the 2D problem these strain fields are written as:

$$\boldsymbol{\varepsilon} = \begin{Bmatrix} \varepsilon_{11} \\ \varepsilon_{22} \\ \varepsilon_{12} \end{Bmatrix}, \quad \boldsymbol{\varepsilon}^{0(11)} = \begin{Bmatrix} 1 \\ 0 \\ 0 \end{Bmatrix}, \quad \boldsymbol{\varepsilon}^{0(22)} = \begin{Bmatrix} 0 \\ 1 \\ 0 \end{Bmatrix}, \quad \boldsymbol{\varepsilon}^{0(12)} = \begin{Bmatrix} 0 \\ 0 \\ 1 \end{Bmatrix}. \tag{10}$$

Finally, rewriting the homogenized elastic tensor as a function of the strain fields, we obtain:

$$\mathbf{E}^H = \frac{1}{|\mathbf{Y}|}\int_Y \mathbf{E}(\boldsymbol{\varepsilon}^0 - \boldsymbol{\varepsilon}^*) dY. \tag{11}$$

where $\boldsymbol{\varepsilon}_{pq}^{*kl} = \frac{1}{2}\left(\frac{\partial \chi_p^{kl}}{\partial y_q} + \frac{\partial \chi_q^{kl}}{\partial y_p}\right)$.

Due to the formulation used in the AH method, it is necessary to integrate Eq. (11) for each element present in the structure in order to obtain the vector of forces and strains. This means that it is necessary to know all the details of the matrices related to the elements, such as the constitutive and strain-displacement matrices. Because of this, each element type will implies in different codes.

Most of the works found in the literature that use AH employ solid elements, since this type of element requires less work in the calculation of the derivatives and in the codification by finite elements of the unit cell (Cai et al., 2014). Another problem related to the method is that for very small elements, such as very thin bars or very thin sheets, even using solid element in the discretization of the members, results in a very large number of elements in the model and thus becomes a time consuming process and, consequently, expensive (Cheng et al., 2013).

3.2 Homogenization of thermal conductivity tensor

Following the same strategy used to obtain the homogenized elastic tensor, the definition of thermal conductivity using index notation is given by:

$$Kt_{ij}^{H} = \frac{1}{|\mathbf{Y}|}\int_{\mathrm{Y}} \left(Kt_{ij} - Kt_{ip}\frac{\partial R^{j}}{\partial y_p}\right) \mathrm{dY}, \tag{12}$$

where Kt_{ij} is the thermal conductivity of material in the unit cell and R^{j} represents the characteristic temperatures of the cell, obtained by:

$$\frac{1}{|\mathbf{Y}|}\int_{\mathrm{Y}} \left[\mathbf{I} - \nabla_{\mathrm{y}}\mathbf{R}(\mathbf{x},\mathbf{y})\right]^{T} \cdot \mathbf{Kt}(\mathbf{x},\mathbf{y}) \cdot \nabla_{\mathbf{y}}\boldsymbol{\delta}\mathbf{T}_1(\mathbf{x},\mathbf{y})\mathrm{dY} = 0. \tag{13}$$

To obtain **R**, the finite element method is used together with the application of periodic boundary conditions on opposite sides of the cell and the system of equations Eq. (14), (15) and (16) is solved analogous the system of equations Eq. (7), (8) and (9), given by

$$\mathbf{CR} = \mathbf{Q}, \tag{14}$$

where **C** is the homogenized stiffness matrix and **Q** is the matrix that covers the global load cases of the system. **C** and **Q** are obtained by:

$$\mathbf{C} = \int_{\mathbf{Y}} \mathbf{B}^{T}\mathbf{KtB}\, dY, \tag{15}$$

$$\mathbf{Q} = \int_{\mathbf{Y}} \mathbf{B}^{T}\mathbf{Kt}\, dY, \tag{16}$$

where **B** is the matrix of the derivatives of the interpolation functions and **Kt** is the thermal conductivity matrix. Thus, Eq. (12) is solved and the homogenized thermal conductivity matrix is obtained (Guth, 2012).

4 THE NOVEL IMPLEMENTATION OF ASYMPTOTIC HOMOGENIZATION METHOD

The novel implementation of the asymptotic homogenization method (NIAH) is based on the mathematical foundation used in the conventional method. However, this method uses commercial finite element software as a black box to obtain the effective properties of the periodic material. In this way, all the finite elements and techniques available in the software can be used to discretize the unit cell.

Thus, starting from the vector of forces of Eq. (9) for the implementation of the new methodology, it is considered that $\boldsymbol{\chi}^{0(kl)}$ as a vector of nodal displacements corresponding to the unit strain field $\boldsymbol{\varepsilon}^{0(kl)}$, thus, we can rewrite Eq. (9) as:

$$\begin{aligned}\mathbf{f}^{kl} &= \int_Y \mathbf{B}^T\mathbf{E}\mathbf{B}\boldsymbol{\chi}^{0(kl)}\,\mathrm{dY} \\ &= \int_Y \mathbf{B}^T\mathbf{E}\mathbf{B}\,\mathrm{d}Y\cdot\boldsymbol{\chi}^{0(kl)} \\ &= \mathbf{K}\boldsymbol{\chi}^{0(\mathrm{kl})}.\end{aligned} \tag{17}$$

This change means that the force vector can be calculated by multiplying stiffness matrix with the displacement field $\boldsymbol{\chi}^{0(\mathrm{kl})}$. With the use of a commercial software, it is only necessary to apply nodal displacements $\boldsymbol{\chi}^{0(\mathrm{kl})}$, run one static analysis and get nodals reactions forces $\mathbf{f}^{kl}$ directly from software's output (Cheng et al., 2013).

Thus, the NIAH procedure starts with the construction of the unit cell model in the finite element software, after this unit displacement fields, called test displacement $\boldsymbol{\chi}^{0(kl)}$ (Eq. (18), are apply fields of unit displacements for the two-dimensional case), are apply on each node of unit cell, after, run static analysis and get nodal reactions forces $\mathbf{f}^{kl}$.

$$\boldsymbol{\chi}_{\mathrm{nó}} = \begin{Bmatrix} u \\ v \end{Bmatrix}, \qquad \boldsymbol{\chi}_{\mathrm{nó}}^{0(11)} = \begin{Bmatrix} x \\ 0 \end{Bmatrix}, \qquad \boldsymbol{\chi}_{\mathrm{nó}}^{0(22)} = \begin{Bmatrix} 0 \\ y \end{Bmatrix}, \qquad \boldsymbol{\chi}_{\mathrm{nó}}^{0(12)} = \begin{Bmatrix} 0.5y \\ 0.5x \end{Bmatrix}, \tag{18}$$

where *x* and *y* are the nodal coordinates in the *x* and *y* directions, respectively.

In the next step, the nodal reaction force $\mathbf{f}^{kl}$ are applied at their respective node together with the application of the periodic boundary conditions at the unit cell boundaries, run again static analysis e get the results the characteristic displacement $\tilde{\boldsymbol{\chi}}^{ij}$. Finally, the characteristic displacements are applied to their respective nodes and get the nodal forces $\mathbf{f}^{*(kl)}$. Thus, with the forces and displacements obtained it is possible to determine the effective elastic tensor, through the equation:

$$E_{ijkl}^{H} = \frac{1}{|\mathbf{Y}|}\left(\boldsymbol{\chi}^{0(ij)} - \tilde{\boldsymbol{\chi}}^{ij}\right)^{\mathrm{T}}\left(\mathbf{f}^{kl} - \mathbf{f}^{*(kl)}\right). \tag{19}$$

The same procedure is performed to obtain the thermal conductivity tensor. But in this case, it is applied temperatures and heat fluxes to perform the analysis. Rewriting the Eq. (16) as a function of the unity thermal gradients, we obtain:

$$\mathbf{q}^{j} = \int_{Y} \mathbf{B}^{T}\ \mathbf{Kt}\ \boldsymbol{\nabla}\mathbf{T}^{0(j)}\, dY, \tag{20}$$

where $\mathbf{q}^{j}$ is the vector of global thermal loads, **Kt** is the thermal conductivity and $\boldsymbol{\nabla}\mathbf{T}^{0(j)}$ are the unit thermal gradients, which for the two-dimensional case are:

$$\boldsymbol{\nabla}\mathbf{T}^{0(j)} = \begin{Bmatrix} \dfrac{\partial T}{\partial x} \\ \dfrac{\partial T}{\partial y} \end{Bmatrix}, \quad \boldsymbol{\nabla}\mathbf{T}^{0(1)} = \begin{Bmatrix} 1 \\ 0 \end{Bmatrix}, \qquad \boldsymbol{\nabla}\mathbf{T}^{0(2)} = \begin{Bmatrix} 0 \\ 1 \end{Bmatrix}. \tag{21}$$

Now, rewriting the Eq. (20) as a function of the unit temperature fields, we obtain:

$$\begin{aligned} \mathbf{q}^{j} &= \int_{Y} \mathbf{B}^{T}\ \mathbf{Kt}\ \mathbf{B}\ \mathbf{R}^{0(j)}\, dY \\ &= \int_{Y} \mathbf{B}^{T}\ \mathbf{Kt}\ \mathbf{B}\, dY \mathbf{R}^{0(j)} \\ \mathbf{q}^{j} &= \mathbf{Q}\ \mathbf{R}^{0(\mathrm{j})}, \end{aligned} \tag{22}$$

where $\mathbf{R}^{0(\mathrm{j})}$ are the temperature fields corresponding to the unit thermal gradients that for the two-dimensional case are:

$$\mathbf{R}^{0(1)} = \begin{Bmatrix} x \\ 0 \end{Bmatrix}, \qquad \mathbf{R}^{0(2)} = \begin{Bmatrix} 0 \\ y \end{Bmatrix}, \tag{23}$$

where *x* and *y* are the global coordinates of each cell node.

Thus, the procedure to find the thermal conductivity through NIAH can be performed: apply the temperature fields $\mathbf{R}^{0(j)}$, run thermal analysis and get the heat flow $\mathbf{q}^{j}$. After, apply the heat flow $\mathbf{q}^{j}$ with the periodic boundary conditions and get the characteristics temperatures $\widetilde{\mathbf{R}}^{*(j)}$. Finally, apply the characteristics temperatures $\widetilde{\mathbf{R}}^{*(j)}$, run thermal analysis and get the corresponding heat flow $\mathbf{q}^{*j}$.

And so, with the values of the heat flows and the temperatures, can be to apply in the equation of the thermal conductivity:

$$Kt_{ij}^{H} = \frac{1}{|\mathbf{Y}|}\left(\mathbf{R}^{0(i)} - \widetilde{\mathbf{R}}^{*(i)}\right)^{T}\left(\mathbf{q}^{j} - \mathbf{q}^{*j}\right). \tag{24}$$

It is noticed that using this novel implementation, all the calculation can be done by a commercial software. In addition, it is not necessary to find the constitutive and strain-displacement matrices for each element. The vector of forces is equal to the vector of nodal reactions, and the strain energy is the multiplication of the vector of nodal reactions by the displacement vectors. All these quantities can be easily obtained from the output of commercial software. Also, all types of elements can be used in the software, without worrying about the detailing of the formulation of the elements (Cheng et al., 2013).

5 OPTIMIZATION

As we are employing the NIAH with a commercial software, the sensitivities are not directly available, then a metamodeling technique is used in the optimization process. The gradient-based SQP algorithm is combined with the Kriging metamodeling technique, obtained from the DACE package developed by Lophaven et al. (2002) in the MATLAB® platform.

5.1 Kriging

Kriging was initially developed for mining and statistical applications involving spatially and temporally correlated data. Mathematically, the Kriging model is composed of a global model $f(\mathbf{x})$ and a local output $Z(\mathbf{x})$:

$$y(\mathbf{x}) = f(\mathbf{x}) + Z(\mathbf{x}), \tag{25}$$

where $y(\mathbf{x})$ is an unknown function of interest, $f(\mathbf{x})$ model the global trend of the function of interest and $Z(\mathbf{x})$ is a stochastic process with mean μ and variance is σ^2.

The term $Z(\mathbf{x})$ provides local deviations, and the covariance between points is given by:

$$Cov\left(Z(\mathbf{x}_i), Z(\mathbf{x}_j)\right) = \sigma^2 \boldsymbol{\Psi}, \tag{26}$$

where $\boldsymbol{\Psi}$ is the correlation matrix defined by the Gaussian correlation function $R(\mathbf{x}_i, \mathbf{x}_j)$, given by:

$$\psi^{(i)} = \exp\left[-\sum_{k=1}^{n} \theta_k \left|x_i^k - x_j^k\right|^2\right]. \tag{27}$$

θ_k are unknown correlation parameters used to find the model, and x_i^k and x_j^k are the *i-th* components of the sampled points $\mathbf{x}_i$ and $\mathbf{x}_j$, respectively.

A new prediction $\hat{y}(\mathbf{x})$, of the responses $y(\mathbf{x})$ at a point $\mathbf{x}$ not sampled is given by:

$$\hat{y}(\mathbf{x}) = \hat{\mu} + \boldsymbol{\psi}^T \boldsymbol{\Psi}^{-1}(\mathbf{y} - \mathbf{1}\hat{\mu}), \tag{28}$$

where $\boldsymbol{\psi}$ is the *i-th* column of $\boldsymbol{\Psi}$ and $\hat{\mu}$ is obtained by:

$$\hat{\mu} = \frac{\mathbf{1}^T \boldsymbol{\Psi}^{-1} \mathbf{y}}{\mathbf{1}^T \boldsymbol{\Psi}^{-1} \mathbf{1}}. \tag{29}$$

One of the greatest advantages found in Gaussian processes is that the model predicts the estimated error of their predictions. In the case of the Kriging metamodel, the estimated error is obtained by:

$$s^2(\mathbf{x}) = \sigma^2 \left[1 - \boldsymbol{\psi}^T \boldsymbol{\Psi}^{-1} \boldsymbol{\psi} + \frac{(1 - \mathbf{1}^T \boldsymbol{\Psi}^{-1} \boldsymbol{\psi})}{\mathbf{1}^T \boldsymbol{\Psi}^{-1} \mathbf{1}} \right]. \tag{30}$$

Equation (30) has the intuitive property that $s^2(\mathbf{x})$ will be zero for any sampled point, this is obvious since for any sampled point there is no uncertainty (Jones, 2001).

5.2 Metamodel-based optimization

A surrogate model or metamodel is a mathematical function of low computational cost used to approximate responses from a more complex and computationally expensive model (Villanueva et al., 2013). The metamodel is generated from a set of initial points obtained by a design of experiments (DOE) strategy. And from its construction, the search process is carried out directly in the metamodel. In this work, the DOE is generated from a Latin hypercube sample (LHS) and, as already mentioned, Kriging is used to build the metamodel. The Kriging response surface is obtained using the DACE package, developed by Lophaven et al. (2002).

The sequential quadratic programming algorithm (SQP) is used optimize the metamodel. This algorithm is chosen because of its efficiency in problems of high and low dimensions. However, this optimizer depends on the guess of the starting point, which can affect your overall search capability. To overcome this disadvantage, a restart technique is used. To perform this technique, it is necessary to add new points to the design space, which aims to increase the accuracy of the model. These new points are obtained by optimizing the Kriging predictor found by the local optimizer. Thus, the optimization algorithm is presented along with the flowchart (Fig. 2):

Algorithm:

1: Generate the sample (**X**) with *m* points using a Latin hypercube;

2: Create the finite element cell model (ABAQUS);

3: Obtain the elastic and thermal properties for sample **X** by NIAH;

4: Evaluate the objective function, **Y** at each point **x** of the sample (**X**);

5: While the stopping criterion is not reached, do:

a) Build Kriging surrogates from **X** and **Y**;

b) Perform the search for the optimal ($\mathbf{x}^*$) of the model from different starting points ($\mathbf{x}_0$) and match the previous points $\mathbf{X} = \mathbf{X} \cup \mathbf{X}(\mathbf{x}^*)$;

c) Get properties by NIAH for $\mathbf{x}^*$;

d) Evaluate the objective function at the optimum point $\mathbf{Y}(\mathbf{x}^*)$ and increment to known values $\mathbf{Y} = \mathbf{Y} \cup \mathbf{Y}(\mathbf{x}^*)$;

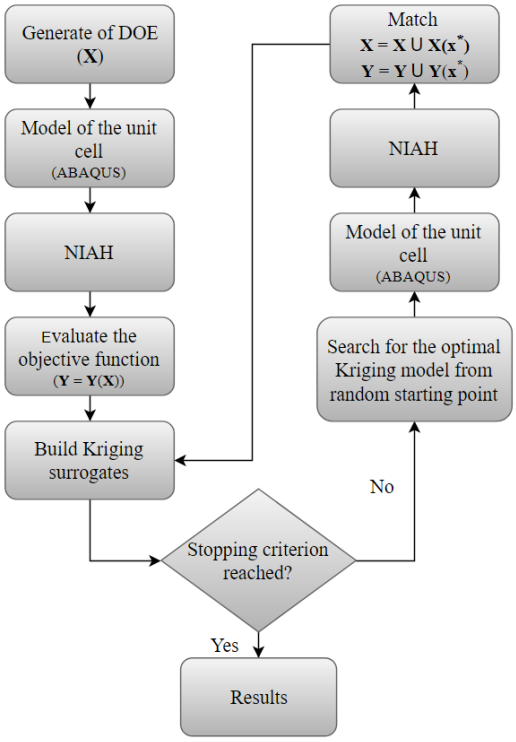

Figure 2. Flowchart of the optimization methodology.

6 RESULTS

In this section, the results regarding the optimization process of lattice cells are presented. In the optimization process, a sequential quadratic gradient-based algorithm is used and the cross-sectional areas are taken as design variables. The implementation of the NIAH method and the finite element modeling of the unit cell is performed in ABAQUS® and the development of the algorithm for calculating elastic and thermal tensors is performed in MATLAB®. Two optimization processes are performed aiming at maximizing the shear modulus and maximizing thermal conductivity in the x direction. The constant relative density is maintained at 49%. In this way, the results obtained by the optimization of the initial cell are presented and compared to those obtained by Guth (2012).

6.1 Initial cell

The initial cell chosen to be optimized is taken from the work of Guth (2012) and it is represented in Fig 3.The cell is modeled using 2D bar elements, where the initial cross-sectional area, modulus of elasticity and thermal conductivity are $A = 1\text{x}10^{-5}\ [m^2]$, $E = 210\ [GPa]$ e $k = 50\ [W/m\ °C]$, respectively. The length of each side of the cell is 0.1 $[m]$. Also in Fig. 3, the elastic and thermal tensors obtained by Guth (2012) using the AH method are presented. The tensors obtained by NIAH, in this work, are presented in Fig. 3, to be compared with the results obtained by Guth (2012). In addition, the polar diagrams for the homogenized components E^H_{1111}, E^H_{1212} and Kt^H_{11} are also presented.

Initial cell

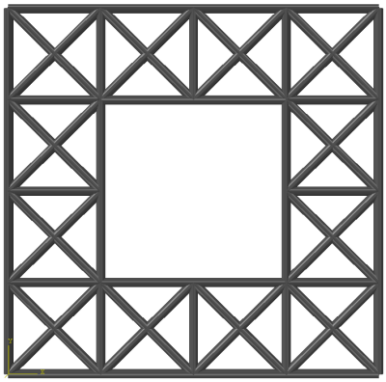

Initial cell

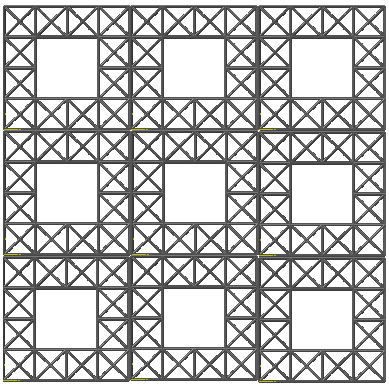

Corresponding material

Results obtained by AH by Guth (2012)

$$\mathbf{E}^H = \begin{bmatrix} 0.1150 & 0.0271 & 0 \\ 0.0271 & 0.1150 & 0 \\ 0 & 0 & 0.0240 \end{bmatrix} [GPa]$$

$$\mathbf{Kt}^H = \begin{bmatrix} 0.0390 & 0 \\ 0 & 0.0390 \end{bmatrix} \left[\frac{W}{m^0 C}\right]$$

Results obtained by NIAH (present study)

$$\mathbf{E}^H = \begin{bmatrix} 0.115003 & 0.027062 & 0 \\ 0.027062 & 0.115003 & 0 \\ 0 & 0 & 0.024045 \end{bmatrix} [GPa]$$

$$\mathbf{Kt}^H = \begin{bmatrix} 0.038967 & 0 \\ 0 & 0.038967 \end{bmatrix} \left[\frac{W}{m^0 C}\right]$$

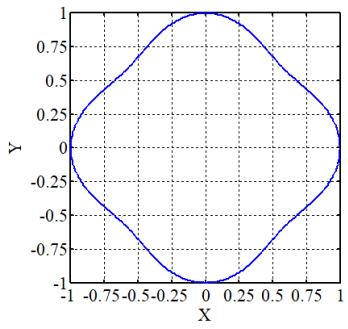

Component E^H_{1111} rotated and normalized by

$E^H_{1111} = 0.115003\ GPa$

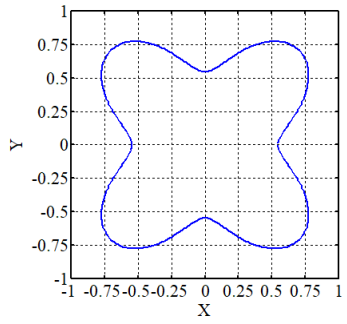

Component E^H_{1212} rotated and normalized by

$E^H_{1212} = 0.043971\ GPa$

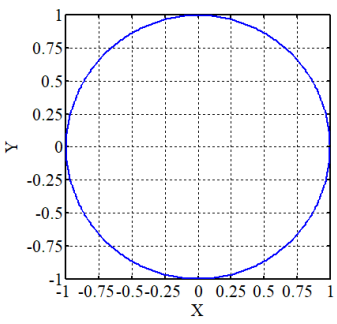

Component Kt^H_{11} rotated and normalized by

$Kt^H_{11} = 0.038967\ W/m°C$

Figure 3. Initial base cell in two dimensions. Font: Guth (2012, p. 62).

6.2 Maximization of the shear modulus

In this case, the E^H_{1212} component of the tensile tensor is maximized and the results are presented in Fig. 4. The increase in the objective function is 3.8 times, resulting in a shear modulus of 91.8 *MPa*. To obtain these results, 300 samples to generate the initial metamodel

(DOE) and more 300 infill points were used. Regarding the corresponding polar plot of Fig. 4, the shear stiffness is maximum at points opposite to the *x* and *y* axes and is zero at 45°. The thermal tensor lost some of its isotropy when compared to the thermal tensor of the initial cell.

In the maximization of the shear modulus, the value find in this work is the same value found by Guth (2012). Despite of this, the cross-sectional areas of the elements of the unit cell find in this work are different those found by Guth (2012). Guth (2012), obtained a unit cell with the same areas for all elements. The areas find here are different for each element. However, the similarity between the cells, can be seen when comparing Fig. 4 and Fig. 5.

Maximization of the shear modulus

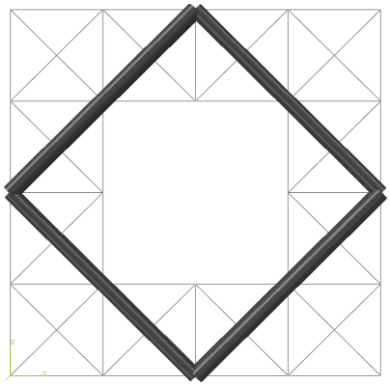

Optimized cell

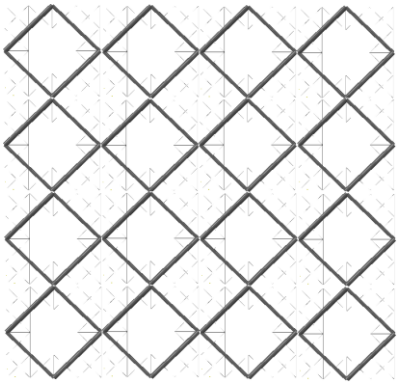

Corresponding material

Results obtained by NIAH

$$\mathbf{E}^H = \begin{bmatrix} 0.091800 & 0.091791 & 0.012945 \\ 0.091791 & 0.091800 & 0.012945 \\ 0.012945 & 0.012945 & 0.091791 \end{bmatrix} [GPa]$$

$$\mathbf{Kt}^H = \begin{bmatrix} 0.043713 & 0.006165 \\ 0.006165 & 0.043713 \end{bmatrix} \left[\frac{W}{m^0 C}\right]$$

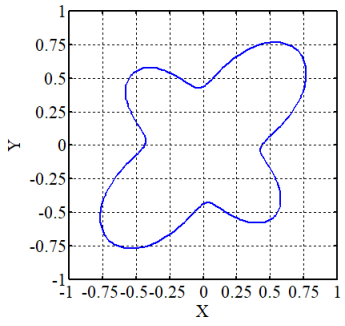

Component E^H_{1111} rotated and normalized by

$E^H_{1111} = 0.209478\ GPa$

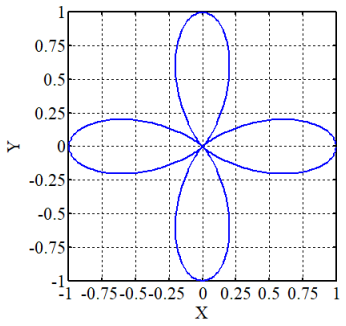

Component E^H_{1212} rotated and normalized by

$E^H_{1212} = 0.091791\ GPa$

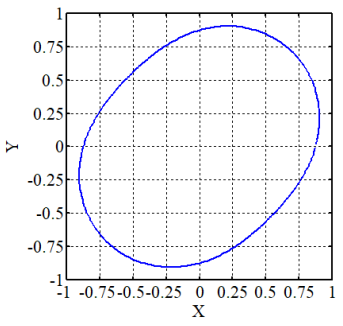

Component Kt^H_{11} rotated and normalized by

$Kt^H_{11} = 0.049877\ W/m°C$

Figure 4. Results of the shear modulus maximization.

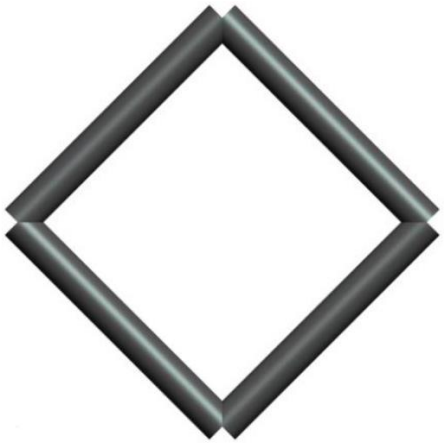

Figure 5. Optimized cell obtained by Guth (2012), maximization the shear modulus. Font: Guth (2012, p.63).

The convergence curve (normalized objective function versus the number of finite element evaluations) can be seen in Fig. 6. The objective function is normalized with respect to the shear modulus of the initial cell.

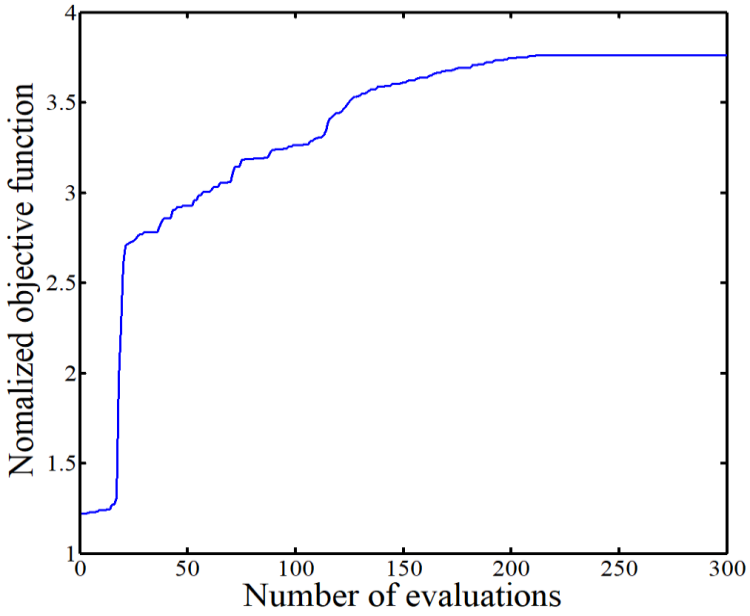

Figure 6. Convergence curve of the normalized objective function for the maximization of the shear modulus.

6.3 Maximization of the thermal conductivity in the x direction

In this problem, the Kt_{11}^{H} component of the thermal conductivity tensor is maximized. The obtained thermal and elastic tensors show that the material has thermal conductivity and elastic stiffness only in the x direction, which is to be expected. This result serves to validate other results, since it is obvious that the higher thermal conductivity must be obtained when the bars align in the x direction. For this problem Guth (2012), obtained a maximum conductivity of 0.0874 *W/m°C* too. However, in his work Guth (2012) obtained greater uniformity in the cross-

sectional areas of the bars with greater thermal conductivity. This can be seen by comparing Fig. 7 and Fig. 8.

Maximization of the thermal conductivity in the x direction

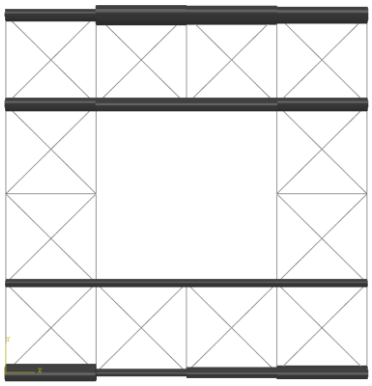

Optimized cell

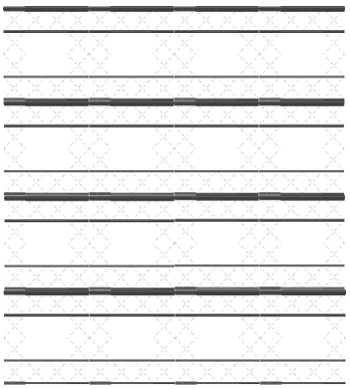

Corresponding material

Results obtained by NIAH

$$\mathbf{E}^H = \begin{bmatrix} 0.367165 & 0.000003 & 0 \\ 0.000003 & 0.000012 & 0 \\ 0 & 0 & 0.000003 \end{bmatrix} [GPa]$$

$$\mathbf{Kt}^H = \begin{bmatrix} 0.087421 & 0 \\ 0 & 0.000004 \end{bmatrix} \left[\frac{W}{m^0 C}\right]$$

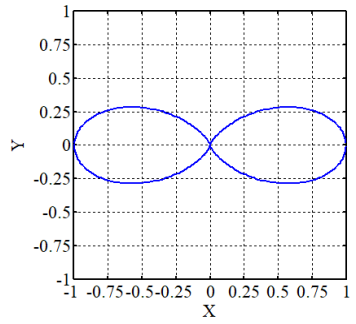

Component E^H_{1111} rotated and normalized by

$E^H_{1111} = 0.367165\ GPa$

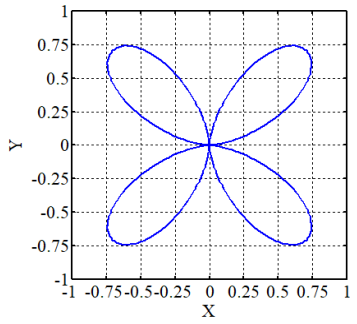

Component E^H_{1212} rotated and normalized by

$E^H_{1212} = 0.091793\ GPa$

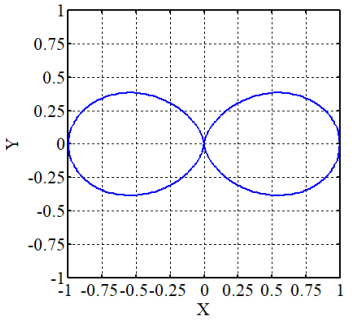

Component Kt^H_{11} rotated and normalized by

$Kt^H_{11} = 0.087421\ W/m°C$

Figure 7. Results of the thermal conductivity maximization.

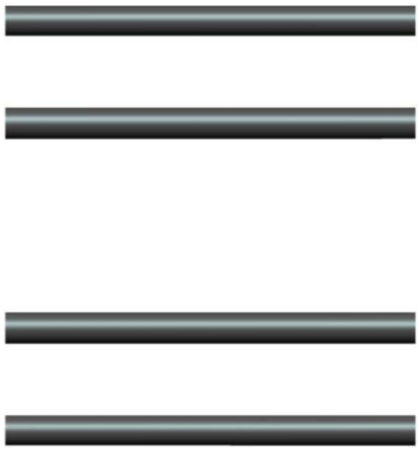

Figure 8. Optimized cell obtained by Guth (2012), by maximization the thermal conductivity in the x direction. Font: Guth (2012, p. 68).

Another important information is how much the objective function improved as a function of the thermal conductivity of the initial cell. This improvement was 2.2 times, and this can be seen in Fig. 9, which shows the increase of the objective function in relation to the number of iterations, normalized as a function of the thermal conductivity of the initial cell. To obtain this improvement, it was used 400 samples to generate the initial metamodel (DOE) and more 400 infill points.

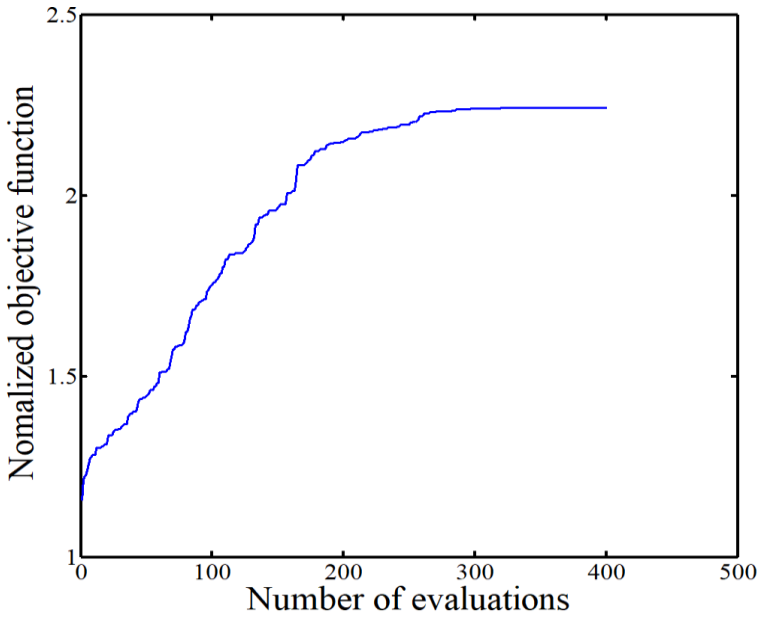

Figure 9. Convergence curve of the normalized objective function for the maximization of thermal conductivity in the x direction.

7 CONCLUSIONS

In this work, the effective properties of each cell is obtained through the new implementation of asymptotic homogenization (NIAH). In the optimization process, the

sequential quadratic programming algorithm is used in the optimization of lattice structures, together with an infill strategy to improve the efficiency of the Kriging metamodel. Two objective functions are studied: the shear modulus and the thermal conductivity in the x direction, for which the cross-sectional areas are used as design variables.

The problem of thermal conductivity maximization in the x direction served to validate other results, noting that the maximum thermal conductivity should be found in the direction along the bars, just as it did.

ACKNOWLEDGEMENTS

The authors would like to thank the Brazilian agencies CAPES and CNPq.

REFERENCES

Ashby, M. F., Evans, A. G., Fleck, N. A., Gibson, L. J., Hutchinson, J. W., Wadley, H. N. G., 2000. *Metal Foams - A design guide.* Elsevier.

Cai, Y., Xu, L. & Cheng, G., 2014. Novel numerical implementation of asymptotic homogenization method for periodic plate structures. *International Journal of Solids and Structures,* vol. 51, n. 1, pp. 284-292.

Cheng, G.-D., Cai, Y.-W. & Xu, L., 2013. Novel implementation of homogenization method to predict effective properties of periodic materials. *Acta Mechanica Sinica,* vol. 29, n. 4, pp. 550-556.

Guedes, J. M.; Kikuchi, N., 1989. Preprocessing and postprocessing for materials based on the homogenization method with adaptive finite element methods. *Computer Methods in Applied Mechanics and Engineering,* vol. 83, n. 2, pp. 143-198.

Guth, D. C., 2012. *Otimização de materiais contituídos de células treliçadas com restrições de isotropia para aplicações termomecânicas.* Programa de Pós Graduação em Ciências e Engenharia de Materiais - PGCEM, Universidade do Estado de Santa Caratina.

Hassani, B. & Hinton, E., 1998. A review of homogenization and topology optimization I—homogenization theory for media with periodic structure. *Computers & Structures,* vol. 69, n. 6, pp. 707-717.

Hassani, B., Hinton, E., 1999. *Homogenization and Structural Topology Optimization - Theory, Practice and Software.* Springer.

Jones, D. R., 2001. A Taxonomy of Global Optimization Methods Based on Response Surfaces. *Journal of Global Optimization,* vol. 21, n. 4, pp. 345-383.

Jones, D. R., Schonlau, M. & Welch, W. J., 1998. Efficient Global Optimization of Expensive Black-Box Functions. *Journal of Global Optimization,* vol. 13, n.4, pp. 455-492.

Lophaven, S. N., Nielsen, H. B., Sondergaard, J., 2002. Aspects of the MATLAB Toolbox DACE. *Informatics and Mathematical Modelling,* p. 44.

Muñoz-Rojas, P. A., Carniel, T. A., Silva, E. C. N. & Öchsner, A., 2010. Optimization of a Unit Periodic Cell in Lattice Block Materials Aimed at Thermo-Mechanical Applications. *Advanced Structured Materials,* vol. 2, n. 1, pp. 301-345.

Roustant, O., Ginsbourger, D. & Deville, Y., 2012. DiceKriging, DiceOptim: Two R Packages for the Analysis of Computer Experiments by Kriging-Based Metamodeling and Optimization. *Journal of Statistical Software,* vol. 51, n. 1, pp. 1-55.

Sigmund, O., 1994. *Design of Material Structures Using Topology Optimization.* PhD thesis, Technical University of Denmark.

Villanueva, D., Haftka, R. T., Le Riche, R., Picard, G., 2013. Locating Multiple Candidate Designs with Surrogate-Based Optimization. *10th World Congress on Structural and Multidisciplinary Optimization*, pp. 1-12.

Wadley, H. N. G., 2002. Cellular Metals Manufacturing. *Advanced Engineering Materials,* vol. 4, n. 10, pp. 726-733.

Zok, F. W., Latture, R. M. & Begley, M. R., 2016. Periodic truss structures. *Journal of the Mechanics and Physics of Solids,* vol. 96, n. 1, pp. 184-203.